Ultrahigh vacuum and high-pressure coadsorption of CO and H_2 on Pd(111): A combined SFG, TDS, and LEED study

Matthias Morkel, Günther Rupprechter,[a] and Hans-Joachim Freund
Fritz-Haber-Institut der Max-Planck-Gesellschaft, Department of Chemical Physics, Faradayweg 4-6, D-14195 Berlin, Germany

(Received 17 June 2003; accepted 26 August 2003)

Sum frequency generation (SFG) vibrational spectroscopy was carried out in conjunction with thermal desorption spectroscopy, low-energy electron diffraction, and Auger electron spectroscopy to examine the coadsorption of CO and H_2 on Pd(111). Sequential dosing as well as various CO/H_2 mixtures was utilized to study intermolecular interactions between CO and H_2. Preadsorbed CO effectively prevented the dissociative adsorption of hydrogen for CO coverages $\geqslant 0.33$ ML. While preadsorbed hydrogen was able to hinder CO adsorption at low temperature (100 K), hydrogen was replaced from the surface by CO at 150 K. When 1:1 mixtures of CO/H_2 were used at 100 K, hydrogen selectively hindered CO adsorption on on-top sites, while above ~ 125 K no blocking of CO adsorption was observed. The observations are explained in terms of mutual site blocking, of a CO–H phase separation, and of a CO-assisted hydrogen dissolution in the Pd bulk. The temperature-dependent site blocking effect of hydrogen is attributed to the ability (inability) of surface hydrogen to diffuse into the Pd bulk above (below) ~ 125 K. Nonlinear optical SFG spectroscopy allowed us to study these effects not only in ultrahigh vacuum but also in a high-pressure environment. Using an SFG-compatible ultrahigh vacuum-high-pressure cell, spectra of 1:10 CO/H_2 mixtures were acquired up to 55 mbar and 550 K, with simultaneous gas chromatographic and mass spectrometric gas phase analysis. Under reaction conditions, CO coverages $\geqslant 0.5$ ML were observed which strongly limit H_2 adsorption and thus may be partly responsible for the low CO hydrogenation rate. The high-pressure and high-temperature SFG spectra also showed indications of a reversible surface roughening or a highly dynamic (not perfectly ordered) CO adsorbate phase. Implications of the observed adsorbate structures on catalytic CO hydrogenation on supported Pd nanoparticles are discussed. © *2003 American Institute of Physics.* [DOI: 10.1063/1.1619942]

I. INTRODUCTION

In order to gain information on adsorbate structures present under atmospheric pressure we have recently investigated the adsorption of CO on supported Pd nanoparticles and Pd single-crystal surfaces over a wide range of pressure and temperature.[1–3] Using sum frequency generation (SFG) vibrational spectroscopy, CO adsorbate structures were monitored from ultrahigh vacuum (UHV) up to 1 bar and it was shown that the high-pressure CO structures were identical to the corresponding high-coverage structures observed under UHV (with ''regular'' on-top, bridge, and hollow bonded CO species). Pre- and post-exposure analysis by low-energy electron diffraction (LEED) and Auger electron spectroscopy (AES) indicated the absence of strong changes in surface morphology and composition upon high-pressure CO exposure. By combining high-pressure x-ray photoelectron spectroscopy (XPS) and SFG,[4] a quantitative analysis of CO coverages up to 1 mbar was performed and it was shown that even at high pressure CO dissociation was absent.

In spite of these results one has to keep in mind, however, that simple extrapolations from low to high pressure may still be incorrect, in particular at elevated temperature. Low- (UHV) and high-pressure gas exposures at a given temperature produce different surface coverages and, even more important, different site occupations. For instance, at 300 K a CO pressure of about 1000 mbar was necessary to reach saturation on Pd(111) while typical UHV studies (10^{-9}–10^{-6} mbar) would be limited to a lower-coverage range. Of course, high coverages can also be obtained under UHV, but typically only at low temperature (~ 100 K), which leads to another complication. The reduced mobility of adsorbed CO at low temperature generates kinetically hindered adsorbate structures, different from the equilibrium phases obtained at high temperature and high pressure. The possible role of such nonequilibrium CO structures for catalysis was discussed in Ref. 5. Consequently, one has to be very careful when transferring low-pressure results to technical conditions and *in situ* measurements are certainly preferable.[6–8]

In the present study we attempt to extend the picture to the coadsorption of CO and H_2 on Pd(111), both at low and elevated (mbar) pressure. The CO–H_2 interaction is not only interesting from a fundamental point of view, but also of relevance for methanol synthesis and decomposition, since the coadsorption of two or more species is an important ini-

[a]Author to whom correspondence should be addressed. Fax: +49 30 8413 4105; Electronic mail: rupprechter@fhi-berlin.mpg.de

tial step in heterogeneous catalysis. Under UHV, the SFG spectra were complemented by LEED, AES, and thermal desorption spectroscopy (TDS), providing additional information on the adsorbed overlayer.

Although CO/H_2 is a relatively simple system, it exhibits a complex behavior due to the large number of well-ordered CO structures on Pd(111) (Refs. 2 and 3, and references therein) and the various states of adsorbed and absorbed hydrogen. A number of effects have been observed in previous studies: e.g., blocking of hydrogen adsorption by CO,[9–11] segregation of CO and H into islands or formation of intermixed layers,[12] displacement of adsorbed H by CO,[11,13–15] changes in the hydrogen desorption temperature upon adsorption of CO,[11] formation of subsurface H and H absorption,[10,16–19] etc. A hydrogen-induced compression of CO and oxygen islands on Pd(111) was observed in recent scanning tunneling microscopy (STM) studies by the Salmeron group.[20,21] $CO–H_2$ interaction was also studied on other metals:[12] e.g., Pt,[22,23] Ir,[24] and Ni.[25,26]

The above-mentioned coadsorption studies were typically carried out by sequentially exposing the reactant molecules (i.e., dosing one type of molecule after the other). This may give rise to strong site blocking unless the coverage of the first molecule is kept very low. In contrast, in the course of a catalytic reaction *a mixture* of reactant molecules typically approaches the catalyst, which may lead to a very different situation. Therefore, to address this issue, we have employed both types of gas exposure (sequential dosing and premixed gases) and, in fact, different adsorption site occupancies were observed. In order to identify adsorbate structures present during CO hydrogenation reactions, various CO/H_2 mixtures were studied in the mbar range at temperatures up to 550 K. This is at least six orders of magnitude higher in pressure than conventional UHV studies and close to conditions used for atmospheric pressure reactions on model or impregnated catalysts. In fact, adsorbate structures different from those present under UHV were observed.

II. EXPERIMENT

A. SFG-compatible UHV-high-pressure cell

The experiments were carried out in a UHV surface analysis system combined with an SFG-compatible UHV-high-pressure cell, as described previously.[2,27] The UHV section (base pressure 1×10^{-10} mbar) is equipped with LEED, AES, and TDS. The sample crystal is spotwelded to two Mo rods and can be resistively heated to 1300 K and cooled with liquid N_2 to 85 K. For SFG spectroscopy, the sample is transferred under UHV to the SFG cell which is equipped with CaF_2 windows. During this operation the sample holder is inserted into an arrangement of three differentially pumped spring-loaded Teflon seals separating the SFG cell from the UHV section, thus allowing experiments to be carried out under UHV or at high pressure (up to 1 bar). Gas phase analysis during atmospheric pressure experiments is performed by gas chromatography (with thermal conductivity and flame ionization detectors) and mass spectroscopy. In order to acquire SFG spectra under UHV, the SFG cell is equipped with its own turbomolecular pump, leak valve, and ionization gauge (which are, of course, separated by gates valves during high-pressure experiments).

B. Vibrational sum frequency generation spectroscopy

SFG spectroscopy has been described in a number of publications.[28–35] Briefly, (picosecond) laser pulses at a tunable infrared frequency ω_{IR} and at a fixed visible frequency ω_{VIS} are spatially and temporally overlapped on the adsorbate/Pd(111) surface. When the IR frequency is scanned over a vibrational resonance of the adsorbate, an SFG signal is generated at the sum frequency ($\omega_{SFG}=\omega_{IR}+\omega_{vis}$). Plotting the SFG intensity versus the IR wave number results in a vibrational spectrum. Since SFG is not allowed in media with inversion symmetry, the SFG signal is mainly generated by adsorbed species, while the centrosymmetric Pd bulk and the isotropic gas phase give only a small contribution to the signal. This guarantees an extreme surface sensitivity even in the presence of a high-pressure gas. For a description of the most important aspects of SFG theory (signal intensity, line shape, selection rules) we refer to Refs. 2 and 35. The current SFG spectra were fitted according to Eqs. (1) and (2) in Ref. 2 and exact values of the resonance frequency and linewidth are indicated in the spectra. High-pressure SFG spectra were corrected for IR gas phase absorption as described in Ref. 2.

The laser setup consisted of a 50 Hz-Nd:YAG laser (1064 nm, 30 mJ/pulse, 20 ps), followed by an SHG (second harmonic generation) unit to produce 532 nm visible light and an OPG-DFG (optical parametric generation and difference frequency generation) unit, which provided the tunable IR light with a resolution of $\sim5\ cm^{-1}$. Pulse energies applied during the experiments were $\sim200\ \mu J$ for the visible and $\sim50–150\ \mu J$ for the IR light (3–6 μm). After passing spatial filters (apertures) and spectral (edge) filters, the generated SFG light was detected by a photomultiplier. Every data point represents an average of 400 laser shots and was normalized to the incident IR and visible energies (typical SFG spectra take about 20 min).

C. Sample preparation and gas dosing

The Pd(111) surface was prepared by cutting and polishing, followed by sequences of flashing to 1250 K, Ar^+ bombardment (700 V at 5×10^{-6} mbar, 5 μA current), annealing to 1250 K, and oxidation between 1200 and 600 K in 5×10^{-7} mbar O_2, followed by a final flash to 1200 K. The surface structure and cleanliness of Pd(111) were confirmed by LEED, AES, and CO-TDS. After similar treatments STM inspection by Mitsui *et al.*[21] revealed a concentration of subsurface impurities (O, C, S) below 1%.

To remove Ni- and Fe-carbonyl impurities, CO (purity $\geqslant$99.997%) was passed over a carbonyl absorber cartridge and then introduced via a cold trap filled with liquid nitrogen. As shown by our previous studies, this cleaning is inevitable for high-pressure experiments.[3,4] Hydrogen (purity $\geqslant$99.9999%) was cleaned using a cold trap. When gas mixtures were used, CO and H_2 were premixed in a glass bulb at

mbar pressures prior to exposure to Pd(111). In this case a baratron gauge was used; for UHV exposures, the pressure indicated by the ionization gauge was corrected by the gauge sensitivity factors for H_2 (0.44) and CO (1.0).

As shown below, in some cases the resulting adsorbate structure strongly depended on the type of gas exposure. The procedure of dosing CO and H_2 is therefore briefly described. After adsorbing the first type of molecule (e.g., CO), SFG, TDS, and LEED measurements were taken. In case of TDS (heating rate 1 K/sec^{-1}) it is apparent that the adsorbate layer (e.g., CO) was removed during the thermal experiment. In this case the exposure of the first type of molecule (e.g., CO) was repeated and immediately followed by exposure of the second type of molecule (e.g., H_2), before a second TDS spectrum was acquired. In the case of (nondestructive) SFG and LEED, after adsorbing the first type of molecule (e.g., CO) and taking measurements the second type of molecule (e.g., H_2) was adsorbed and the measurements were repeated. In addition, measurements were recorded after subsequently dosing the two molecules (without intermittent measurement) but no differences were detected. When TDS spectra are reported in the literature, the spectra are frequently ''background'' corrected; i.e., any mass signals originating from the ''clean'' surface due to adsorption of residual gas molecules are subtracted. We have deliberately avoided that procedure and report ''uncorrected'' mass spectra because even small amounts of adsorbed molecules could already induce site blocking. CO coverages were calculated by integrating TDS areas, using the (2×2) 0.75 ML CO structure as reference.

III. RESULTS AND DISCUSSION

In this section, we present coadsorption experiments using different types of gas exposure (sequential and mixtures) focusing on the mutual site blocking between CO and H_2. Results from pure CO adsorption are briefly repeated to allow for an easier comparison. Finally, the interaction of CO and H_2 at high pressure is described.

A. CO adsorbate structures

SFG spectra of CO on Pd(111) from 10^{-8} to 1000 mbar and between 100 and 500 K have been presented in detail in preceding papers.[2,3,5] In agreement with earlier infrared reflection absorption spectroscopy (IRAS), LEED, and TDS studies (e.g., Refs. 36–40) several well-ordered structures were observed: e.g., a $(\sqrt{3}\times\sqrt{3})R30°$-1CO at 0.33 ML, a $c(4\times2)$-2CO at 0.5 ML, a $(4\sqrt{3}\times8)$rect at 0.63 ML, and a (2×2)-3CO at 0.75 ML [1 ML equals the density of Pd atoms in the (111) plane, 1.53×10^{15} cm^{-2}].

Each CO adsorbate structure exhibits a characteristic SFG vibrational spectrum and LEED pattern, as illustrated by Fig. 1. CO initially adsorbs in fcc threefold hollow sites with stretching frequencies around 1850 cm^{-1} at 0.33 ML (see, e.g., Fig. 1 of Ref. 3). At 0.5 ML, a peak at 1920 cm^{-1} is observed [Fig. 1(a)] which is generally assigned to CO in fcc and hcp threefold hollow sites.[41–43] However, in a recent STM study Rose *et al.*[20] were able to show that near $\theta=0.5$ two types of $c(4\times2)$ structures coexist: one with CO in fcc and hcp threefold hollow sites and one with bridge-bonded $c(4\times2)$ (as originally suggested by vibrational spectroscopy[37]). In the range between 0.5 and 0.6 ML the CO peak continuously shifts to higher wave numbers [Fig. 1(b)]. Above $\theta=0.6$, CO is preferentially bridge bonded ($\sim$1960 cm^{-1}) with a smaller amount of linear (on-top) CO at 2075–2085 cm^{-1} whose intensity is very sensitive to coverage [Figs. 1(c) and 1(d)]. If the coverage is further increased, the bridge site intensity decreases, the on-top signal increases, and a transition[40] from a bridge–on-top structure to a hollow–on-top structure occurs. At saturation $(2\times2,\ \theta=0.75)$, two bands at 1899 and 2108 cm^{-1} (fcc and hcp hollow and on-top CO) are observed [Fig. 1(f)].

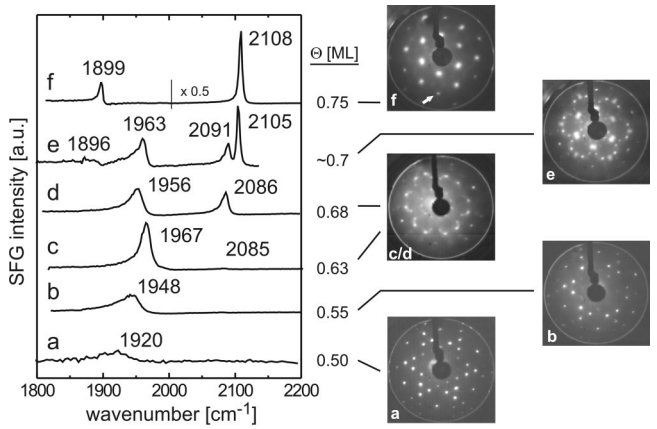

FIG. 1. SFG spectra and corresponding LEED patterns of various CO structures on Pd(111) (CO coverage indicated). The adsorbate layers can be produced by the following CO exposures: (a) 10^{-6} mbar at 350 K or 1 L at 95 K, (b) 10^{-6} mbar at 250 K or 2 L at 95 K, (c) 10^{-6} mbar during cool down from 300 to 190 (measurement without background gas) or 3–5 L at 95 K, (d) 10^{-6} mbar during cool down from 300 to 190 (measurement with background gas), (e) 10^{-7} mbar during cool down from 300 to 90 K or 5–10 L at 90 K, and (f) 10^{-6} mbar during cool down from 300 to 90 K; see text. The LEED pattern in (e) is a superposition of patterns (c), (d), and (f). In the LEED pattern (f) one Pd substrate spot is marked with an arrow.

Coverages (θ) in Fig. 1 were obtained from TDS measurements. Due to the lower sensitivity of SFG to multiple-bonded CO, the CO coverage cannot be simply deduced from integration of the SFG peak areas (for details see Refs. 2 and 3). Since the infrared and Raman transition moments are different for different adsorbate geometries (e.g., hollow versus linear-bonded CO) and may even depend on coverage,[44] the sensitivity of SFG towards different adsorbate species is different, hence making a quantitative analysis difficult. However, for CO/Pd(111) the strong coverage dependence of the C–O stretching frequency (Fig. 1) allows a good estimation of the actual CO coverage, which was recently confirmed by our combined high-pressure SFG and XPS measurements.[4]

The formation of well-ordered structures is facilitated by exposing CO at $\geqslant$250 K and cooling to the desired temperature, as reported in Refs. 3, 5, 40, and 45. Otherwise, ''non-equilibrium structures'' may be obtained, such as the one shown in Fig. 1(e) exhibiting hollow (1896 cm^{-1}), bridge (1963 cm^{-1}), and two on-top CO peaks (2091 and 2105 cm^{-1}). SFG and LEED revealed a superposition of domains with coverages of 0.63–0.68 ML [Figs. 1(c) and 1(d)] and of 0.75 ML [Fig. 1(f)]. Previous studies[5] have shown

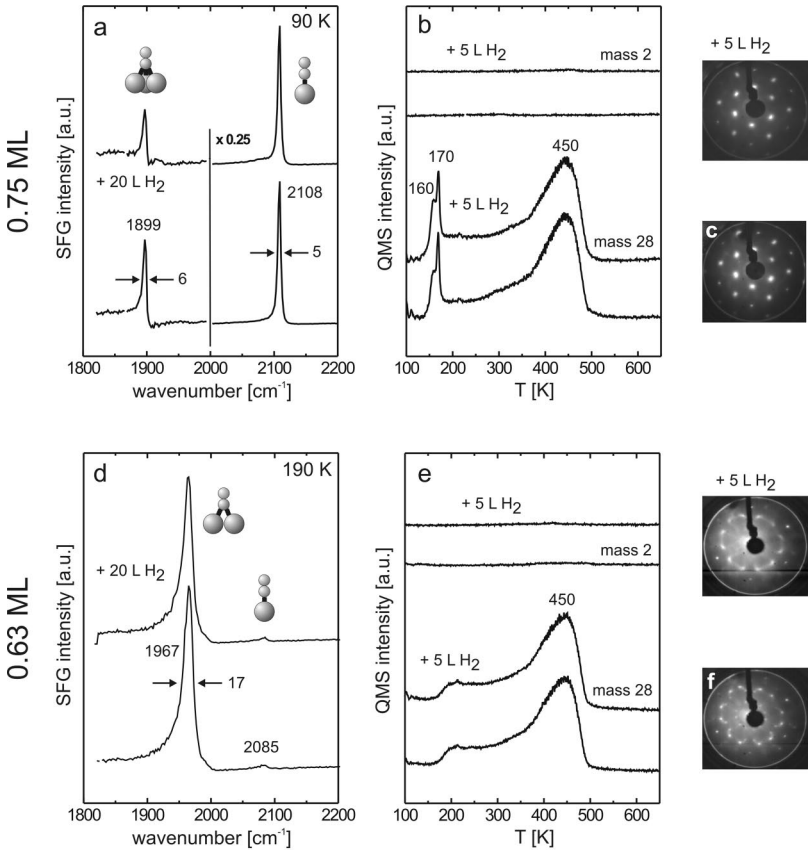

FIG. 2. Sequential dosing of CO and H_2 on Pd(111): A CO coverage of 0.75 ML was prepared by cooling Pd(111) in 3×10^{-6} mbar CO from 300 to 90 K and characterized by SFG (a), TDS (b), and LEED (c) (lower traces and lower LEED pattern). After adsorbing 5–20 L hydrogen at 90 K the measurements were repeated [(a)–(c), upper traces and upper LEED pattern]. The same experiment was also carried out starting with a 0.63 ML CO structure (d)–(f).

that the formation of a well-ordered (2×2) saturation structure requires a sufficiently high CO mobility (temperatures of $\sim$150 K to overcome the CO diffusion barrier) and a sufficient CO flux (e.g., $\sim10^{-6}$ mbar at 150 K) to avoid ''quenching'' of domains with lower coverages. In the following, conditions have therefore been selected to avoid nonequilibrium structures (e.g., by cooling the sample from ca. 300 K to 100 K in the respective gas) and to produce more homogeneous adsorbate layers.

B. Sequential dosing of CO and H_2

1. CO followed by H_2

Of course, CO/H_2 coadsorption has already been studied in the past and site blocking effects have been reported.[9–11] However, for completeness and to allow a better comparison with following data, SFG, TDS, and LEED measurements acquired after CO exposure on Pd(111) and after subsequent H_2 exposure are collected in Fig. 2.

After saturating Pd(111) with CO by cooling in 3×10^{-6} mbar CO from 300 to 90 K (to avoid nonequilibrium structures), SFG and LEED indicated the formation of a well-ordered $(2\times2$, 0.75 ML) hollow–on-top-CO structure with narrow peaks at 1899 and 2108 cm^{-1} (full width at half maximum of 6 and 5 cm^{-1}, respectively) [Figs. 2(a) and 2(c)]. The cooling takes about 6 min—i.e., the total CO exposure amounts $\sim$1000 L (langmuir: 10^{-6} mbar sec). The coverage of 0.75 ML is also evident from the CO-TDS spectrum (mass 28) in Fig. 2(b) displaying two characteristic sharp low-temperature peaks at 160 and 170 K (originating from the hollow–on-top to bridge–on-top phase transition upon desorption[40]), and from the major CO desorption peak at 450 K. The H_2-TDS (mass 2) spectrum indicated that there was no hydrogen adsorption from the residual gas.

If up to 20 L hydrogen were then dosed at 90 K on the CO-precovered (0.75 ML) Pd(111) surface [Figs. 2(a)–2(c)], no changes were observed by SFG, CO-TDS (mass 28), or LEED. The H_2-TDS (mass 2) spectrum confirmed that there was no hydrogen adsorption under these conditions [Fig. 2(b)]. It should be noted that on the clean Pd(111) surface already less than 1 L hydrogen at 90 K is sufficient to produce a pronounced hydrogen desorption signal [similar to the one shown in Fig. 3(b); see, e.g., also Refs. 11 and 46]. Apparently, hydrogen was unable to adsorb on the CO-precovered surface; i.e., the surface sites for dissociative hydrogen adsorption were blocked by CO. In light of the dense structure of the preadsorbed CO layer (0.75 ML), this observation is not surprising and has been reported previously (e.g., Refs. 9–11).

Site blocking may occur through several mechanisms which can be hardly disentangled.[12] For instance, the sites for dissociative hydrogen adsorption may be occupied by CO or they may be vacant but made inaccessible due to the presence of neighboring CO molecules. Dong and Hafner[47] have studied the dissociative adsorption of H_2 on Pd(111) by total energy calculations and have identified a variety of dissociation pathways and sites. Six possible dissociation pathways were reported that were either nonactivated or slightly activated (involving different adsorption geometries of the H atoms in the H_2 molecule adsorbing in fcc, hcp, bridge, and top sites) and only the top-top path (both H atoms adsorb on

on-top sites) did not lead to a stable dissociation state (for illustrations see Ref. 47). Although the (2×2) (0.75 ML) structure is dense with three CO molecules in the unit cell (two hollow, one on-top), in a simple geometric picture three on-top, six bridge sites, and six hollow sites would be still available in the unit cell, allowing for several of the hydrogen adsorption configurations suggested by Dong and Hafner [due to due to its small size, H–H distance 0.74 Å (Ref. 48), the hydrogen molecule would geometrically fit in between the CO molecules if Pauli repulsion is neglected]. However, it is clear from the observed suppression of hydrogen adsorption that such a purely geometric picture is oversimplified.

One has to rather consider that preadsorbed CO modifies the electronic structure of the substrate (i.e., increasing the barrier for hydrogen adsorption), in particular when the CO molecules are densely packed with pronounced intermolecular interactions, which are evident from the strong dipole coupling in vibrational spectra [cf. the large frequency shifts in SFG spectra with coverage in Fig. 1 (Refs. 2 and 3)]. This ''electronic site blocking'' is particularly well known for sulphur, which induces a reduction of CO (Ref. 49) or hydrogen (Ref. 50) adsorption that is much higher than expected from a purely geometric site blocking. For CO on Pd(111), 0.4–0.5 ML S reduced the CO uptake $\sim$15 times.[49] In the case of hydrogen, 0.33 ML sulfur completely blocked H_2 adsorption.[51] This effect can be explained by the influence of sulfur on the electronic structure of the substrate which increases the barrier for dissociative hydrogen adsorption at or near the sulfur atom. A similar poisoning is known for C, O, P, and Cl (Ref. 52) and a theoretical study of the effect of such adsorbates was carried out by Norskov *et al.*[53] For preadsorbed CO, Eriksson and Ekedahl[13] reported that below a CO coverage of 0.18 ML hydrogen dissociation was nonactivated while above 0.18 ML CO a linear increase in the hydrogen dissociation barrier (and in the hydrogen desorption energy) was found. On Ir(111), 0.15–0.20 ML of preadsorbed CO reduced the saturation coverage of deuterium at least 4 times.[24]

Because the hindering of hydrogen adsorption should decrease with decreasing CO coverage, we have also prepared CO layers of smaller coverage. When the Pd(111) surface was precovered with 0.63 ML CO (by cooling in 3×10^{-6} mbar CO from 300 to 190 K, then switching off the CO background pressure), SFG exhibited a bridge peak ($1967\ cm^{-1}$) and a weak on-top peak ($2085\ cm^{-1}$), while LEED showed the characteristic ''flower'' pattern [Figs. 2(d) and 2(f)].[2] In TDS the phase transition peaks at 160 and 170 K (that only occur for 0.75 ML) were absent [Fig. 2(e)]. After subsequent hydrogen exposure at 190 K no changes were again observed by SFG and TDS; i.e., H_2 adsorption was still inhibited [the somewhat blurred LEED pattern in Fig. 2(f) after hydrogen exposure is due to electron beam damage; see Fig. 3 in Ref. 2]. Hydrogen inhibition persisted for CO layers with even lower coverages (e.g., $\sim$0.55 ML CO, not shown). Kok *et al.*[11] reported that no hydrogen adsorbed when Pd(111) was fully covered with a $(\sqrt{3}\times\sqrt{3})R30°$ CO structure (0.33 ML, in the following denoted ''$\sqrt{3}$''). On the time scale of the SFG experiment (20–30 min), we have observed a (partial) conversion of the $\sqrt{3}$ structure to the $c(4\times2)$-2CO (0.5 ML) structure. It was not possible to disentangle exactly, if the $\sqrt{3}$ to $c(4\times2)$ transformation originated from a real increase in CO coverage (CO adsorption from the residual gas) or from hydrogen adsorption inducing a (partial) compression of the $\sqrt{3}$ CO domains as reported in an STM study by Rose *et al.*[20] (both CO and H_2 are present in the residual gas of a UHV chamber). However, the hydrogen-induced compression seems less likely in our case because it requires free Pd areas in between $\sqrt{3}$ CO islands. At (total) CO coverages below 0.33 ML, CO already forms islands in the $(\sqrt{3}\times\sqrt{3})R30°$ structure (local coverage 0.33 ML).[54] TDS spectra by Kok *et al.*[11] show that (after CO adsorption at 220 K) hydrogen can adsorb on the (clean) Pd(111) areas between the CO islands and, resulting from repulsive interactions, CO and H segregate into separate islands.[12,20] In case of separate islands, CO and H_2 desorb independently from each other [H_2 desorption around 300 K; cf. Fig. 3(b)].[11]

Summarizing, CO coverages of 0.33 ML and above were very effective to prevent dissociative hydrogen adsorption, presumably due to increasing the barrier for dissociative hydrogen adsorption. Purely geometric effects cannot explain the observed site blocking, not even for high coverages. A very similar site blocking was also observed for ''nonequilibrium'' CO structures (see Ref. 5). When a mixture of domains with 0.75 and 0.63–0.68 ML coverage [cf. Fig. 1(e)] were exposed to 50 L H_2, no changes in the spectrum occurred, indicating that there was no rearrangement and redistribution of the CO domains and H_2 adsorption was effectively blocked.

2. H_2 followed by CO

As shown in the previous section, hydrogen adsorption is strongly hindered when preadsorbed CO is present. Because for a reaction proceeding via a Langmuir–Hinshelwood mechanism the adsorption of both reactants is required, we have reversed the dosing sequence to ''guarantee'' that adsorbed hydrogen is present on the Pd surface. However, as shown below, even in that case hydrogen is not necessarily located on the Pd surface. When H_2 exposure was followed by CO, the resulting adsorbate structures turned out to be strongly dependent on the temperature of the Pd(111) substrate.

Figure 3 collects SFG, TDS, and LEED measurements of CO adsorption on H-precovered Pd(111) at 100 K and 150 K, together with results obtained from the hydrogen-saturated surface. We will first discuss the effect of hydrogen (pre)adsorption. When the Pd(111) surface was cooled from 300 K to 100 K in 1×10^{-7} mbar H_2 (ca. 100 L), the subsequent H_2-TDS spectrum (mass 2) showed a hydrogen desorption peak at $\sim$295 K due to recombinative desorption of surface hydrogen and of hydrogen from subsurface and bulk sites [Fig. 3(b)].[10,46,55] About 30% of the desorbing hydrogen originates from the Pd bulk, producing a high-temperature tailing (this assignment will be discussed in detail below). Adsorbed hydrogen could not be detected by SFG (the Pd–H stretch vibration is outside our SFG frequency range[56]) and also the LEED pattern in Fig. 3(c) indicated no change when compared to the (1×1) pattern of clean Pd(111) (Ref. 16)

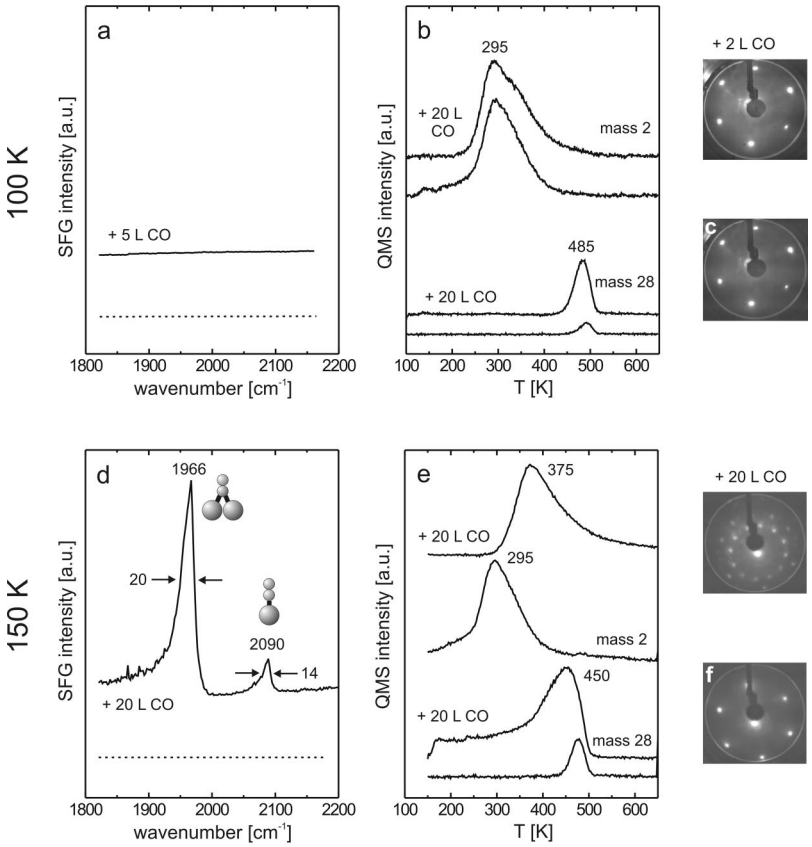

FIG. 3. Sequential dosing of H_2 and CO on Pd(111): After cooling Pd(111) in 1×10^{-7} mbar H_2 from 300 K to 100 K, SFG (a), TDS (b), and LEED (c) measurements were taken (lower traces and lower LEED pattern). After adsorbing 5–20 L CO at 100 K the measurements were repeated [(a)–(c), upper traces and upper LEED pattern]. The same experiment was also carried out with a hydrogen preexposure between 300 K and 150 K with measurements taken before [(d)–(f), lower traces and lower LEED pattern] and after CO exposure [(d)–(f), upper traces and upper LEED pattern].

[suggesting a (1×1)-H structure]. The CO-TDS spectrum in Fig. 3(b) showed a small peak at 485 K, which may be due to several reasons. One possibility is that CO from the residual gas may adsorb when the Pd(111) surface is cooled from 700 to 300 K after sample preparation and/or during H_2 exposure from 300 K to 90 K (total ca. 7 min). The amount of CO seems to be very small because one does not observe an SFG signal or LEED pattern. A second contribution may originate from CO adsorbing during the TPD run while and after the hydrogen is desorbing (based on our temperature ramp, there are 3 min between 150 and 450 K). Assuming a total time of ca. 10 min and a CO pressure of $1-2\times10^{-10}$ mbar, an upper limit of 0.1 ML CO may originate from background adsorption. As mentioned above, at such low CO coverages hydrogen is able to adsorb on Pd(111) (as obvious from the 295 K H_2 desorption peak). Given that the CO molecules form islands,[20] the majority of the Pd surface is clean when hydrogen arrives; i.e., the overall influence of background CO adsorption should be negligible.

When up to 20 L CO were subsequently dosed at 100 K, SFG did still not detect any CO resonances between 1700 and 2200 cm^{-1} [Fig. 3(a)]. LEED did also not exhibit any CO superstructure and only the background increased slightly [Fig. 3(c)]. The CO-TDS spectrum (mass 28) still showed a small desorption peak, which, as described above, is rather related to CO adsorption from the residual gas. It should be noted that on a clean Pd(111) surface an exposure of 2 L CO would be sufficient to produce a coverage of at least 0.6 ML. Apparently, H preexposure at 100 K led to a strong inhibition of CO adsorption.[10,24]

If the same experiment was repeated at 150 K [Figs. 3(d)–3(f)], no differences were observed after H_2 adsorption (surface cooled from 300 K to 150 K in 1×10^{-7} mbar H_2, ca. 50 L). No (CO) SFG resonance was detected, a (1×1) LEED pattern was observed, and the H_2-TDS spectrum (mass 2) was identical to that in Fig. 3(b). However, a different structure was observed after CO adsorption. When the hydrogen-precovered Pd surface was exposed to 20 L CO at 150 K, SFG showed signals due to bridge (1966 cm^{-1}) and on-top (2090 cm^{-1}) bonded CO, typical of a CO coverage around 0.65 ML.[2,3] An ordered structure was observed by LEED [Fig. 3(f)], which can also be attributed to CO structures in the 0.6–0.7 ML range. This is further corroborated by the CO-TDS (mass 28) indicating a CO coverage of 0.70 ML (note that the 160 and 170 K peaks, typical of 0.75 ML, are absent). The (upper) CO-TDS trace in Fig. 3(e) is identical to a CO-TDS without preadsorbed hydrogen, suggesting that surface hydrogen is absent; i.e., there is a complete removal of surface hydrogen by CO. The H_2-TDS after CO exposure now had its maximum at 375 K; i.e., the peak was shifted by 80 K to higher temperature. This rules out the possibility that CO and H_2 were present as separate islands on the surface because in that case hydrogen should still desorb around 300 K. The size of the H_2-TDS peak was nearly unchanged (ruling out hydrogen desorption upon CO exposure) but the high-temperature tailing was more pronounced. The measurements indicate that at 150 K CO removes and replaces hydrogen from the surface and most likely pushes the hydrogen below the surface. The shape of the H desorption peak with its high-temperature tailing, characteristic of diffusion-controlled desorption kinetics, further

supports this assumption [similar peak shapes were described by several authors, e.g., on Pd(111) (Ref. 46), Pd(110) (Refs. 9 and 10), and Pd(100) (Refs. 19 and 57)]. The LEED pattern showing a dense CO layer (with no space for H) also suggests that H moved below the surface.

Apparently, preadsorbed hydrogen hindered CO adsorption at 100 K but was replaced from the surface by CO at 150 K. In the following, we will discuss possible explanations for this behavior. As mentioned above, the H_2-TDS spectra after adsorbing 10^{-7} mbar H_2 between 300 and 100 K and between 300 and 150 K were identical, so different hydrogen coverages are not responsible (TDS spectra of 2 L hydrogen at 90 K and 150 K were identical, not shown). The temperature-dependent site blocking ability of hydrogen is rather related to the state of adsorbed and absorbed hydrogen at the different exposure temperatures. Hydrogen adsorption and absorption on Pd single-crystal surfaces has been studied by many techniques (for a review see, e.g., Refs. 48 and 58). Different types of hydrogen species were observed: i.e., surface hydrogen, subsurface hydrogen (populating sites between the first and second layers of the substrate), a near-surface hydride (accumulating in a region of up to 4 nm depth), and bulk hydrogen located deeper in the Pd bulk, forming a homogeneous solution of H in the metal lattice. A common observation is that the relative abundance of the different H species strongly depends on the adsorption temperature (and somewhat on the history of the sample; how long the crystal is held *in vacuo* after H exposure, etc.).

Using TDS, Gdowski *et al.*[46] studied the effect of different hydrogen exposure temperatures. At 80 K a single desorption peak (β) was observed at ~310 K and attributed to the occupation of surface threefold hollow sites as well as octahedral sites between the first and second layers.[55] For adsorption between 90 and 140 K and large exposures (ca. 100–10000 L), a new (α) TDS peak appeared at ~170 K which was attributed to the decomposition of a near-surface palladium hydride. The population of this α state was thermally activated with a maximum at ca. 115 K. Above 140 K, the α state disappeared while the total amount of absorbed H increased strongly due to hydrogen dissolution in the Pd bulk (leading to an additional state, later termed α_2,[10,19] producing the high-temperature tail).

Taking into account the observations by Gdowski *et al.*[46] and others (discussed below) we suggest the following picture to explain the presence (absence) of CO blocking by hydrogen at 100 K (150 K). At 100 K, hydrogen adsorbs on surface and subsurface Pd sites. This is supported by *I-V* LEED and total energy calculations,[55,59–61] showing that surface fcc hollow sites and subsurface octahedral sites are the preferred adsorption sites [$(\sqrt{3}\times\sqrt{3})R30°$-2H structure with up to 67% subsurface population]. Although there is some debate if ''subsurface'' occupation is limited to the first and second layers of the substrate or may include ''near-surface'' regions (of ca. 4 nm depth[57]), it is clear that no pronounced hydrogen absorption and dissolution deep in the Pd bulk occur at 100 K because the activation barrier for H dissolution cannot be overcome. Consequently, at 100 K preadsorbed H is restricted to the surface and subsurface (or near-surface) region, thus preventing any CO adsorption. By contrast, at 150 K preadsorbed hydrogen can be replaced by CO due to the ability of thermally activated H to move below the surface into deeper Pd layers—i.e., to dissolve in the Pd bulk.

Previous experimental studies of hydrogen adsorption using a variety of techniques support this explanation. The different adsorption and absorption properties of H at low (100 K) and high (~250 K) temperature were studied by Eberhardt *et al.* using angle-resolved photoemission.[62,63] Adsorption of hydrogen on Pd(111) at 100 K produced a bonding H level split off from *d* bands with H atoms bound in threefold surface sites. However, warming the adsorbed layer to or exposing at near room temperature caused an irreversible conversion of H into a (lower-energy) binding site where the split-off state was no longer visible and the *d*-like surface states were unaffected. It was suggested that penetration of H below the Pd(111) surface to be responsible for the loss of H-induced features in UPS. Under similar conditions, Kubiak and Stulen[64] reported a decrease in electron-stimulated desorption yield upon heating the sample to temperatures below the onset of desorption and suggested that hydrogen diffused into regions many layers below the Pd surface. On Pd(100), combining nuclear reaction analysis and TDS Wilde *et al.*[57] reported that below 130 K hydrogen was chemisorbed at the surface (saturating at 1.0 ML) with a small fraction of further dosed hydrogen penetrating the surface and accumulating in a region of up to 4 nm depth (i.e., not only in the first-layer subsurface sites). Above 130 K, H migration from such a near-surface hydride phase to the deeper Pd bulk occurred, leading to solution of H in Pd.

CO-induced hydrogen absorption, desorption, and dissolution were reported for several surfaces, but typically at temperatures of 200 K and above. Upon H_2/CO coadsorption at 220 K, Kok *et al.*[11] observed a high-temperature hydrogen desorption peak (~430 K). It was suggested that during the growth of CO islands H atoms become trapped within the CO islands or may be pushed below the surface. As similar effect was observed by Behm *et al.*[10] on Pd(110) and by Nyberg *et al.*[56] on Pd(100) reporting H dissolution in the bulk upon CO adsorption. Nyberg *et al.*[56] also reported a (near-)surface hydride [with a characteristic electron energy loss spectroscopy (EELS) peak at 56 meV], which disappeared upon heating to 250 K due to hydrogen dissolution in the bulk.

Eriksson and Ekedahl[13] performed very elegant real-time measurements of hydrogen desorption and absorption when CO was dosed onto a hydrogen-precovered polycrystalline Pd thin film using a Pd-MOS device. By measuring the capacitance-voltage characteristics of the Pd-MOS device and, in parallel, by taking mass spectra of desorbing molecules it could be clearly shown that a CO exposure of a hydrogen-precovered Pd surface at 223 K yielded a simultaneous desorption and absorption of adsorbed hydrogen. The amount of hydrogen absorption depended on the relative rates of hydrogen desorption and of CO adsorption (i.e., it depended on surface temperature and CO pressure). These authors have also suggested a driving force for the H dissolution. For hydrogen, steady-state conditions are obtained faster between the bulk and surface than between the surface and gas phase, because the energy barrier between surface

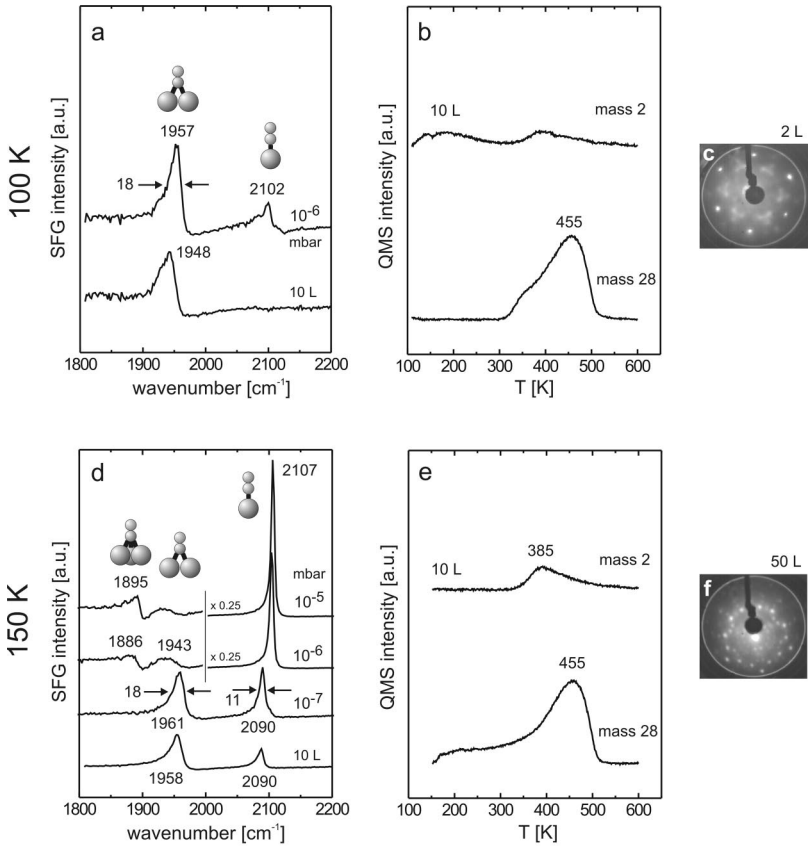

FIG. 4. Exposing a 1:1 CO/H_2 mixture to Pd(111): SFG, TDS, and LEED measurements were taken after exposure at 100 K (a)–(c) and at 150 K (d)–(f); exposure and pressure conditions are indicated.

and bulk is about a factor of 2 smaller than the desorption energy.[13] Consequently, if the CO adsorption rate is larger than the hydrogen desorption rate, a temporary increase in the local hydrogen coverage may be obtained, leading to an increased hydrogen concentration (dissolution) in the Pd bulk. In the measurements of Eriksson and Ekedahl[13] at 223 K the hydrogen desorption rate is about four orders of magnitude lower than the CO adsorption rate at 10^{-8} Torr CO, leading to an increased hydrogen dissolution in the Pd bulk. Accordingly, hydrogen dissolution is even more favored at the conditions of our experiment: i.e., 150 K and 10^{-7} mbar CO.

Based on the various experimental observations, the temperature-dependent site blocking ability of hydrogen can be explained by dissolution of surface and subsurface (near-surface) hydrogen in the Pd bulk upon CO adsorption at 150 K. This picture also explains the high-temperature hydrogen desorption peak after CO adsorption at 150 K [Fig. 3(e)]. Hydrogen located in the Pd bulk can only desorb after (partial) CO desorption from the Pd surface. The onset temperature of hydrogen desorption can be understood by considering that recombinative H_2 desorption can only take place after enough CO has desorbed to produce a sufficient free Pd surface. From integrating the CO-TDS area up to the onset of the 375 K H_2 desorption peak, we estimate that a CO coverage of less than 0.55 ML is needed for recombinative H_2 desorption. At the maximum H_2 desorption (375 K), the CO coverage was about 0.3 ML.

Summarizing, it should be noted that the site-blocking ability of hydrogen was strongly temperature dependent. At 100 K, hydrogen was inhibiting CO adsorption because the energy barrier to hydrogen bulk dissolution cannot be overcome; i.e., hydrogen stays on the surface and near the surface and blocks CO. At 150 K, CO was able to replace hydrogen from the surface which moved to deeper Pd layers. In the next section on CO/H_2 mixtures, we present further evidence for this picture.

C. Dosing of CO/H_2 mixtures

In the preceding sections it was shown that the mutual site blocking of CO and H_2 strongly depended on the dosing sequence and the exposure temperature. At 100 K, preadsorbed CO fully prevented hydrogen adsorption and vice versa; i.e., under these conditions only one type of molecule was present on the surface. However, in the course of a catalytic reaction, a mixture of reactant molecules is exposed to the catalyst, which should allow the simultaneous presence of both reactant molecules. To address this topic, CO and H_2 were premixed in a glass bulb prior to exposure to Pd(111). As shown below, conditions can be found where CO and H_2 coexist on the surface and where the structure of the CO layer is strongly modified by hydrogen.

When 10 L of a 1:1 CO/H_2 mixture were dosed at 100 K [Fig. 4(a)], the resulting SFG spectrum exhibited a single peak at 1948 cm^{-1} (bridge-bonded CO) while on-top CO was absent. This already indicates a strong interaction of CO and H_2 because an exposure of ~ 5 L (pure) CO would produce a dense nonequilibrium CO structure (0.7 ML), including a large on-top peak as shown in Fig. 1(e). After increasing the pressure to 1×10^{-6} mbar CO/H_2 a small signal in the on-top region occurred, but its intensity was only $\sim 5\%$

of that in a ''normal'' 0.7 ML CO structure, again indicating a strong CO–H_2 interaction. The CO-TDS in Fig. 4(b) acquired after the 10 L exposure indicated a CO coverage of about 0.55 ML and LEED [Fig. 4(c)] showed a $c(4\times2)$-like ordering, suggesting a $\sim$0.5 ML coverage in agreement with CO-TDS. Two small, broad H_2 desorption peaks were found around 170 K and 370 K. Based on calibration measurements with pure H_2 (assuming that 1 L H_2 at 90 K produces a coverage of ca. 0.7 ML, not shown[55]), the total amount of both H_2 peaks is $\sim$0.2 ML.

Apparently, under conditions when CO and H_2 simultaneously approach the Pd(111) surface, intermolecular interactions produce ''new'' adsorbate structures, the absence or strong reduction of on-top bonded CO being the most striking finding. Hydrogen seems to prevent CO from adsorbing at on-top sites or steers the CO layer in a configuration that does not include on-top CO. Taking into account previous vibrational studies[22,23,25] and recent STM data of CO, O_2, and H_2 interactions on Pd(111) by Rose and co-workers,[20,21] we suggest the following model to explain our observation.

When a CO/H_2 mixture is dosed on Pd(111) at 100 K, CO and hydrogen form separate islands due to the frequently reported repulsive interaction between CO and H_2, and CO forms a $c(4\times2)$ structure at $\sim$0.5 ML including bridge (hollow) bonded CO. Surprisingly, the CO coverage seems to be limited to $\sim$0.5 ML (as evident from our SFG and TDS spectra and LEED) and the CO islands do not adopt a 0.75 ML (2×2) structure with hollow and on-top CO. This is in full agreement with the STM results by Rose *et al.*[20] reporting that when CO and H_2 coexisted on Pd(111), hydrogen was able to compress a $\sqrt{3}$ CO layer into a $c(4\times2)$ structure but not to a (2×2). For a reason yet unknown, coadsorbed hydrogen seems to destabilize the (2×2) structure or, at least, on-top bonded CO.

The ''destabilization'' of on-top CO upon hydrogen adsorption has also been observed for other noble metals. While only on-top CO is normally present on Pt(111) for average CO coverages $<$0.25 ML, using infrared reflection absorption spectroscopy (IRAS) Hodge *et al.*[22] observed that upon H_2 exposure between 100 and 180 K on-top CO decreased and broadened and bridge-bonded CO appeared. A shift of CO from on-top to bridge sites upon H coadsorption also occurred on Pt(335).[23] A similar effect was reported by Zenobi *et al.*[25] for Ni(111) where bridge and on-top CO species coexist for CO coverages below 0.5 ML. Upon exposure to above 10^{-3} mbar H_2 the terminal CO species disappeared and CO was compressed into a disordered phase containing only bridge-bonded CO. EELS studies by Andersson on Ni(100) have also shown a displacement of CO from on-top to bridge sites.[65] According to these and our observations, coadsorbed hydrogen seems to destabilize on-top CO and displace it onto bridge sites. One may argue that this interaction is difficult to understand, considering that CO and H_2 are located in different islands. However, it is possible that the CO–H_2 interaction at the island boundaries is ''passed on'' to inner island regions. In fact, Rose and co-workers[20,21] observed by STM that the hydrogen-induced compression of CO (or oxygen) structures started at the island edges and proceeded towards the island center.

A point to clarify concerns the H_2-TDS spectrum in Fig. 4(b). The broad desorption feature around 170 K [Fig. 4(b)] is presumably related to the $\alpha_{(1)}$ peak reported by Gdowski *et al.*;[46] i.e., it may be due to the decomposition of a near-surface hydride (but the exact origin is still unclear). The observation that there is no surface hydrogen desorption around 300 K appears, at first sight, to be in contradiction with our assumption of the presence of surface hydrogen. However, the TDS spectrum can be explained if surface hydrogen present at 100 K (partly) moves below the Pd surface upon increasing the temperature during TDS. Hydrogen from deeper Pd regions would then desorb after the CO coverage has decreased below 0.55 ML, similar to the situation in Fig. 3(e). Since the total CO coverage is only 0.55 ML, the onset of CO and H_2 desorption is nearly at the same temperature. This picture is again supported by the STM measurements of Mitsui *et al.*[21] who observed that hydrogen disappeared from Pd(111) upon heating, as evident from the reversal of the hydrogen-induced compression of an oxygen layer around 200 K [relaxed from a $(\sqrt{3}\times\sqrt{3})$ to a (2×2) structure]. Since no hydrogen desorbs at this temperature, this observation can only be explained if hydrogen moved to subsurface or deeper sites.

Our explanation is based on the assumption of the phase separation of CO and H_2 due to the repulsion of the two molecules (both CO and H behave as electron acceptors, competing for the substrate electrons). Although we strongly favor this picture due to its agreement with many previous experimental observations, for completeness we also want to discuss other possible explanations. For instance, a mixed CO–H layer may be formed in which on-top sites are not populated. Although this picture may explain the H_2-TDS spectrum (again, the CO coverage must fall below a certain value to allow recombinative H_2 desorption) [Fig. 4(b)], it seems unlikely in light of the repulsive interaction between CO and H_2 (and one may expect a different CO-TDS). One could also speculate that hydrogen located below the Pd surface may influence the CO layer on the surface by destabilizing on-top CO (also in this case, hydrogen can only desorb recombinatively after enough CO has desorbed). However, as shown in Fig. 3(e) even a large amount of hydrogen below the Pd surface did not affect the CO layer on the surface.

In the preceding section (hydrogen adsorption followed by CO adsorption) it was shown that the site blocking of hydrogen vanished at higher temperatures [cf. Figs. 3(d)–3(f)]. Similarly, when 10 L of a CO/H_2 mixture were dosed at 150 K, an SFG spectrum was observed with a bridge peak at 1958 cm^{-1} and an on-top peak at 2090 cm^{-1}, indicating a coverage of 0.68 ML [Fig. 4(d)]. In contrast to the corresponding measurement at 100 K [Fig. 4(a)], the on-top site was now clearly populated. Apparently, hydrogen was no longer able to hinder CO to adsorb on on-top sites. The structure is identical to a pure CO exposure and there are no indications of any hydrogen on the surface. LEED [Fig. 4(f)] also pointed to a 0.68 ML CO structure. CO-TDS indicated a CO coverage of $\sim$0.7 ML and a small hydrogen desorption peak occurred around 370 K. The hydrogen desorption peak originates from hydrogen absorbed to deeper Pd regions or pushed subsurface by CO and is again due to the recombi-

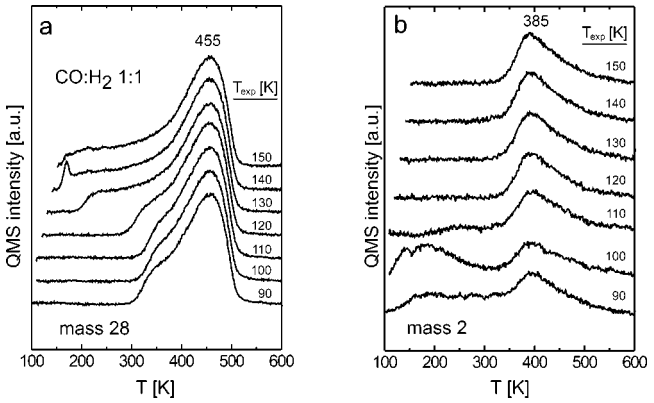

FIG. 5. Thermal desorption spectra of CO (mass 28) and hydrogen (mass 2) acquired after exposing Pd(111) to 10 L CO/H_2 (1:1) mixture at temperatures between 90 and 150 K.

native hydrogen desorption starting after the CO coverage has fallen below ~ 0.5 ML.

Increasing the pressure of the CO/H_2 mixture up to 10^{-5} mbar [Fig. 4(d)] produced higher CO coverages and finally a phase transition to the (2×2) CO superstructure with two bands at 1895 and 2107 cm^{-1} (fcc and hcp hollow and on-top CO) was observed [Fig. 4(d)]. The broad bridge peak at 1943 cm^{-1} indicates that domains with slightly lower coverage were also present. Apparently, the small amount of H below the Pd surface had no effect on the CO surface layer.

Both the experiments with preadsorbed hydrogen and CO/H_2 mixtures have shown that the site blocking of hydrogen (i.e., its ability to stay on the surface) strongly depended on the exposure temperature. In order to exactly determine the ''transition'' temperature at which hydrogen is able to move from the surface to deeper (bulk) Pd regions, we have heated Pd(111) in 10^{-6} mbar CO/H_2 stepwise from 100 K to 150 K. When hydrogen leaves the surface, the CO islands are no longer restricted to the $c(4\times2)$ structure and reorganize to the (2×2) structure. The ''transition'' occurred already at 125 K, which can be easily detected by SFG due to the strong on-top peak of the (2×2) structure. As control experiment, we have also determined the ''transition'' by TDS, exposing 10 L CO/H_2 mixtures at temperatures between 90 and 150 K (Fig. 5). The CO-TDS in Fig. 5(a) shows that the blocking effect of hydrogen was active up to ~ 120 K, limiting the CO coverage to about 0.55 ML (at these temperatures 5 L pure CO would produce 0.7 ML). At 130 K and higher, CO coverages of 0.6–0.73 ML were observed, indicating the absence of a hydrogen-induced site blocking [the small peak in the 140 K trace indicates a near-saturation coverage; cf. Fig. 2(b)].

The H_2-TDS in Fig. 5(b) is a bit more complex because, as described above, part of the surface hydrogen may move below the Pd surface during the TPD run. The H_2-TDS is, therefore, not necessarily characteristic for the initial state of adsorbed hydrogen. After exposing 10 L CO/H_2 mixture at 90 and 100 K, CO and H separate and H adsorbs in surface and subsurface (near-surface) sites, producing two desorption features in TDS. The broad peak around 175 K is probably due to the decomposition of a near-surface hydride. The second peak around 370 K (with a high-temperature tail) is due to hydrogen desorbing from deeper Pd areas, populated presumably during the TPD run. Due to this effect, the temperature at which hydrogen leaves the surface cannot be clearly deduced from H_2-TDS. For instance, while after CO/H_2 exposure at 120 K, CO-TDS shows a site-blocking effect by hydrogen, the corresponding H_2-TDS is already identical to the 150 K trace (where CO-TDS shows no site blocking).

Summarizing the results on CO/H_2 mixtures, we have shown that the resulting adsorbate structures strongly depended on the exposure temperature. At temperatures below about 125 K, hydrogen remained on the surface, thereby blocking and destabilizing on-top CO and limiting the CO coverage within CO islands to ~ 0.5 ML. Above 125 K, CO was able to replace surface hydrogen which moved into the Pd bulk, finally leading to pure CO layers. This replacement is relatively rapid. For a 1:1 CO/H_2 mixture the hydrogen impingement rate is about 4 times higher than the CO impingement rate; i.e., the probability that an empty site is populated by hydrogen is 0.8 and 0.2 for population with CO (assuming that adsorption proceeds via a single collision on a vacant site, neglecting any precursor states). However, because a hydrogen atom can move below the surface while a CO molecule stays on the surface, after five collisions the probability that the surface site is populated by hydrogen is $\sim 30\%$ (i.e., the CO coverage would be ~ 0.65 ML, leading to strong site blocking). At 10^{-6} mbar the hydrogen replacement would only last 1 sec (the impingement rate for the mixture is $\sim 5\times10^{15}/cm^{-2}$ sec) assuming that this effect is limited by CO adsorption rather than hydrogen dissolution.

D. CO/H_2 interaction at high pressure

In the preceding sections we have shown that the adsorbate structures strongly depended on the type of CO and H_2 exposure (sequential versus mixture) and also on the surface temperature. This demonstrates that great care has to be taken when comparing typical UHV (sequential) coadsorption studies at low temperature with catalytic reactions where both molecules interact simultaneously with the catalyst at high temperature.

The current commercial methanol synthesis is based on $Cu/ZnO/Al_2O_3$ but (promoted) Pd catalysts have also been found to be highly selective (e.g., Ref. 66 and references therein). As a first step to get some insight into the adsorbate structure during CO hydrogenation on Pd(111) we have therefore studied the CO/H_2 interaction at elevated pressure up to 550 K. Our conditions are, of course, still different from the 10–25 bar pressures used in technical catalysis but very similar to those of atmospheric pressure reactions on model[49,67–69] or impregnated catalysts.[70]

In a previous publication[2] we have reported SFG spectra of 1:1 CO/H_2 mixtures at 298–523 K that were similar to pure CO spectra with a CO coverage of 0.5–0.6 ML. Because no shifts in the CO frequencies were observed, we had suggested that the interaction of CO and H_2 should be rather weak. However, based on the results presented in this article, the observed (high-coverage) structures can now be rather

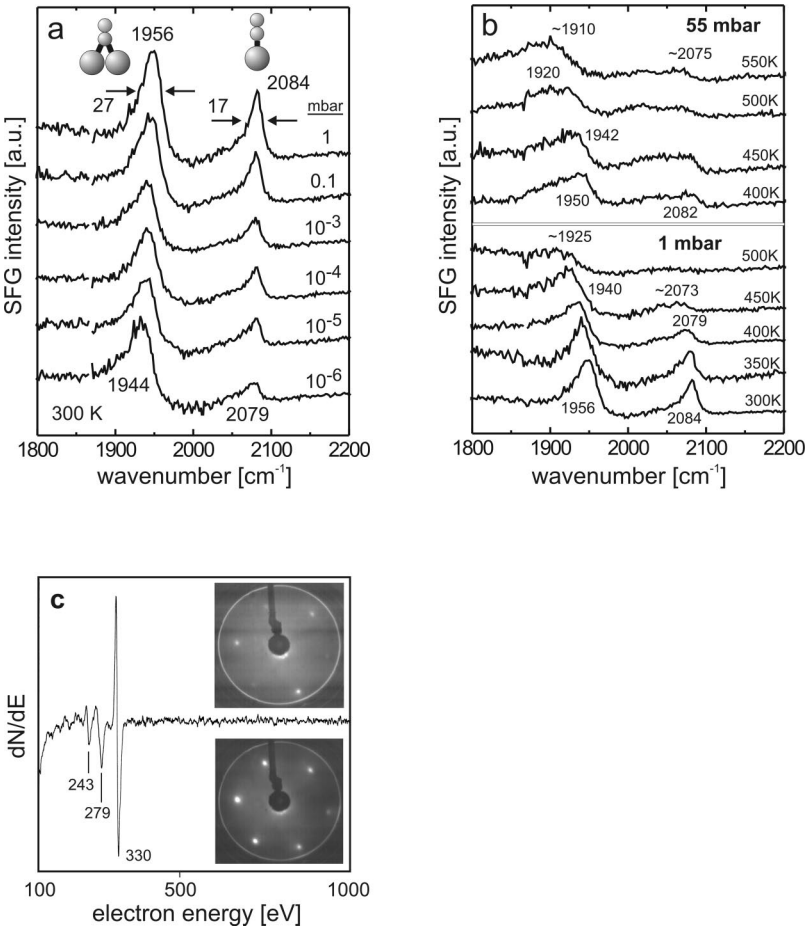

FIG. 6. (a) SFG spectra acquired during room temperature exposure of Pd(111) to a 1:10 CO/H_2 mixture between 10^{-6} and 1 mbar. (b) SFG spectra taken at increasing pressure up to 55 mbar and increasing temperature up to 550 K; see text. LEED patterns in (c) were recorded before (lower) and after (upper) high-pressure gas exposure. The ''post-reaction'' AES spectrum (c) indicates that the surface remained clean during 6 h of gas exposure.

attributed to the strong site-blocking effect of CO; i.e., no hydrogen was present on the Pd(111) surface. In order to facilitate hydrogen adsorption we have therefore utilized a 1:10 CO/H_2 mixture for the current experiments. The high-pressure SFG experiments in Fig. 6 were carried out using CO/H_2 mixtures up to 55 mbar, at a total pressure of 1 bar using He as buffer gas. Figure 6(a) shows the effect of increasing the pressure of a 1:10 CO/H_2 mixture on Pd(111) at 300 K from 10^{-6} to 1 mbar. At 10^{-6} mbar a bridge ($1944\,cm^{-1}$) and on-top ($2079\,cm^{-1}$) CO peak was observed indicating a CO coverage above 0.6 ML. Increasing the pressure to 1 mbar shifted the bridge peak to $1956\,cm^{-1}$ while the on-top signal increased and shifted to $2084\,cm^{-1}$ (typical of a CO coverage of ca. 0.65 ML). When compared to spectra of pure CO adsorption (cf. Fig. 6 in Ref. 2), no significant differences can be observed for the 1:10 CO/H_2 mixture. This indicates that even with a tenfold excess of hydrogen, hydrogen adsorption is strongly inhibited by CO. As expected from the experiments described in the previous sections, when CO and H_2 reach the Pd surface at 300 K they compete for the vacant surface sites. However, since hydrogen can easily move from the Pd surface to subsurface and bulk sites, the vacant sites are more and more populated by CO (even though the hydrogen impingement rate is about 40 times that of CO: see below). Once the CO coverage reaches ~ 0.3 ML, hydrogen adsorption fully stops. It is clear that under these conditions of elevated pressure and temperature a dynamic equilibrium between adsorbed and gas phase molecules is established, as shown by the fast exchange of isotopically labeled CO (see Fig. 13 in Ref. 2). However, when a hydrogen atom desorbs the resulting empty site can be occupied by CO, while an empty site produced after CO desorption is still blocked for hydrogen by the neighboring CO molecules.

The lower panel in Fig. 6(b) shows spectra acquired during heating the Pd(111) surface in 1 mbar 1:10 CO/H_2 mixture stepwise to 500 K. The bridge peak was shifted from $1956\,cm^{-1}$ at 300 K to $1940\,cm^{-1}$ at 450 K, while the on-top signal shifted from $2084\,cm^{-1}$ to $2073\,cm^{-1}$. The frequency shifts are comparable to those in Fig. 6(a) observed with decreasing pressure and coverage. However, increasing the temperature from 300 to 450 K of 1 mbar 1:10 CO/H_2 not only led to a decreasing coverage but also to an increase in the linewidth of the bridge ($27-50\,cm^{-1}$) and on-top ($17-35\,cm^{-1}$) CO species. At 500 K a broad bridge peak around $1925\,cm^{-1}$ was detected, typical of a ~ 0.5 ML CO coverage. Similar observations with, of course, higher CO coverages at a given temperature were made when the pressure of the 1:10 CO/H_2 mixture was increased to 55 mbar [upper panel in Fig. 6(b)]. In that case, the CO layer could be observed up to 550 K, with the bridge peak at $\sim 1910\,cm^{-1}$ again indicating a relatively high CO coverage (around 0.5 ML) and a very broad on-top peak around $2075\,cm^{-1}$. Similarly, SFG spectra of CO/H_2 up to 1000 mbar (1:3; without buffer gas) also indicated CO coverages $\geqslant 0.5$ ML.

When the SFG spectra in Fig. 6(b) (upper panel) are

compared to those of 5 mbar (pure) CO at 300–550 K (not shown), no pronounced differences can be found. The increase in linewidth in Fig. 6(b) is therefore mainly due to a temperature-induced line broadening[37] and a strong effect of hydrogen seems to be absent. The combined effect of a reduced CO coverage and of an increased linewidth at the highest temperatures made the SFG signals very broad and weak, limiting the quality of the SFG spectra (the SFG intensity is proportional to the square of the adsorbate concentration and to the square of the inverse linewidth).

However, one point that should be noted in the high-temperature CO/H_2 spectra, which was also raised in our previous paper,[2] is the appearance of a broad on-top signal (around $2075\,cm^{-1}$) when the bridge signal is found at $1920\,cm^{-1}$ or lower [Fig. 6(b), 55 mbar spectra at 500 and 550 K]. This is not observed in low-temperature CO spectra (cf. Fig. 1 or Fig. 1 of Ref. 3) when a peak at $1900–1920\,cm^{-1}$ ($\leqslant 0.5$ ML) is *not* accompanied by an on-top signal (the on-top signal typically appears only after the CO frequency is shifted to $\sim 1940\,cm^{-1}$ or higher; at CO coverages $\geqslant 0.6$ ML). The broad on-top signal may indicate a roughening of the surface under reaction conditions but this roughening must be reversible because regular CO spectra and LEED images were obtained after removal of the high-pressure gas and decreasing the temperature. Another origin of the broad on-top signal could be a highly dynamic and not perfectly ordered CO phase that is only present during the high-pressure and high-temperature experiment (featuring a distribution of local coverage and/or island size). Taking into account a destabilizing effect of hydrogen on on-top CO, an additional influence of hydrogen leading to smaller and broadened on-top peaks can also not be excluded.

The high-pressure SFG experiments were typically carried out over several hours: therefore, one has to confirm that the Pd surface remains clean during this time. This is only possible by using feed gas that was carefully cleaned from contaminants, as described in previous papers.[3,4] Figure 6(c) displays a LEED pattern and an AES spectrum, taken after 6 h of high-pressure gas exposure. LEED still indicated a six-fold symmetry of the Pd surface (excluding strong restructuring) and AES showed a clean Pd surface without Ni or Fe contamination. Due to the overlap of carbon and Pd AES signals at 272 eV, the presence of very small amounts of carbon cannot be excluded though.

We have tried to detect possible products of CO hydrogenation, such as methanol or methane by gas chromatographic (GC) and mass spectroscopic (MS) detection. Beside the conditions used in Fig. 6, reactions were carried out up to 1000 mbar CO/H_2 (1:3; without buffer gas), at temperatures up to 550 K. Under these conditions, the thermodynamic limit of methanol production at 500–550 K is about 1–0.1 mbar methanol (using equilibrium constants K_p [$K_p = p(CH_3OH)/p(CO)\cdot p^2(H_2)$] of about 6×10^{-3} and $1\times10^{-3}\ bar^{-2}$ for 500 and 550 K, respectively[71,72]). These pressures would be in the range of our GC and MS detection. However, it should be noted that under the applied conditions the rate of (unpromoted) Pd is very small [turnover frequency (TOF) on the order of $5\times10^{-4}\ sec^{-1}$ for 1000 mbar CO/H_2 (1:4–1:2) at 550 K (Refs. 66, 68, 70, and 73)], and in light of the small amount of Pd surface available ($\sim 0.5\,cm^{-2}$), a methanol (or methane) pressure of only $\sim 6\times10^{-4}$ mbar can be produced in our reaction cell after 6 h (which is below the GC detection level). Possible products were therefore condensed and collected in a smaller volume cold trap at 77 K, which should produce a pressure of ~ 0.03 mbar methanol (which would be sufficient for mass spectroscopic analysis). However, no methanol was detected by MS and only minute amounts of CO_2 were found (CH_4 cannot be condensed sufficiently due to its high vapor pressure at 77 K). These traces may originate from CO dissociation and the subsequent reaction of atomic oxygen with CO. However, as shown by LEED and AES the amount of CO dissociation must be very small. In view of our previous high-pressure XPS and SFG study [0.1 mbar CO up to 500 K (Ref. 4)] where no CO dissociation was found on Pd(111) it seems likely that ''side reactions'' with the reactor walls, the thermocouple, etc., may be involved.

The absence of any reaction products is somewhat puzzling. Even though the amount of products would be small under the given conditions, they should still be detectable. However, in a similar study of CO hydrogenation on Pd foil ($\sim 8\,cm^2$) using a low-volume all-glass high-pressure cell[74] and a zeolite cold trap, reaction products were absent as well.[75] Berlowitz and Goodman[68] reported methanol production on Pd(110) at pressures from 0.7 to 2.4 bars using reaction times of ~ 24 h but it was also reported that small amounts of Ni-carbonyl contamination could not be avoided on that timescale.

On the other hand, the absence of products is in line with the high-pressure SFG spectra. Even with a tenfold excess of hydrogen and temperatures up to 550 K the spectra indicated a CO coverage of $\geqslant 0.5$ ML; i.e., this is still in a regime where our UHV coadsorption studies revealed a strong hydrogen inhibition. CO and H_2 were simultaneously exposed to the clean Pd(111) surface but the replacement of hydrogen by CO is again fast. For 1:10 CO/H_2 the hydrogen impingement rate is about 37 times higher than the CO impingement rate (leading to a probability that an empty site is populated by hydrogen of $\sim 97\%$), but after 40 collisions the probability that a surface site is populated by hydrogen has fallen below 30%. At 10^{-6} mbar this would last about 10 sec (impingement rate of the mixture $\sim 4\times10^{15}/cm^{-2}$ sec) which is still faster than the timescale of our SFG setup and at 1 mbar$\sim 10^{-5}$ sec.

The absence of methanol is therefore most likely related to the inability of hydrogen to adsorb on Pd. Vice versa, the strong site blocking of hydrogen by CO may be *responsible* for the low CO hydrogenation rate on Pd. Higher temperatures (lower CO coverages) would be necessary to reduce the site blocking of CO but since methanol synthesis is exothermic[71,72] higher temperatures further reduce the equilibrium concentration of methanol (which is why 525–575 K is the technically interesting range).

In light of our results it is surprising that CO hydrogenation works at all on technical catalysts: e.g., silica supported Pd nanoparticles.[66,70,76–78] Of course, in ''real'' systems the total CO/H_2 pressure (10–25 bars) is 25–500 times higher but the reaction temperature (525–550 K) and the

CO/H_2 ratio ($\sim 1:2$) are similar. As shown in Fig. 6(a) (and, e.g., in Fig. 4 of Ref. 3), increasing the pressure by six or more orders of magnitude induced only relatively small changes in the absolute CO coverage. Therefore, increasing the total pressure of the CO/H_2 mixture 25–500 times may not induce too strong changes in the adsorbate layer (except from increasing the coverage). In fact, the IR spectra reported by Hicks and Bell[78] also show a high CO coverage on Pd nanoparticles on silica under reaction conditions. Increasing the pressure from 1 to 200 bars has also only little effect on the methanol equilibrium constant K_p (increases less than 10 times due to nonideality of gases).[72]

Under technical conditions there may be further effects facilitating the reaction. The most apparent difference is, of course, that the reaction is carried out on supported Pd nanoparticles. On Pd particles exhibiting nanosize facets, on which the formation of well-ordered structures is limited when compared to a macroscopic single-crystal surface, the site-blocking effects may be less pronounced. In addition, the presence of facets other than (111) and step, edge, and corner sites provides new geometries for $CO–H_2$ interaction. For pure CO adsorption on Pd nanoparticles on Al_2O_3,[1–3] we have demonstrated the importance of specific binding sites located on the steps and edges of metal nanoparticles which may lead to inherent differences to Pd(111). In addition, H_2-TDS spectra of Pd nanoparticles are quite different from those of Pd(111), indicating a higher abundance of weakly bound hydrogen on Pd nanoparticles (cf. Ref. 79). The oxide support (e.g., SiO_2, Al_2O_3, TiO_2, MgO, ZnO, etc.) may also participate actively. Although the discussion on the exact role of the support in the hydrogenation reaction may still be controversial (Ref. 71 and references therein), strong support effects on the activity and selectivity are well established[73,78] and possible intermediates such as formate bound to the oxide were detected by secondary ion mass and IR spectroscopy (e.g., Refs. 80 and 81). Studies of CO/H_2 coadsorption on Pd nanoparticles supported on Al_2O_3 are therefore in the focus of our current interest.

Another difference concerns the state of hydrogen. In our experiments we have avoided the formation of β-Pd hydride which would be accompanied by a recrystallization of the Pd(111) crystal (and thereby destroy its well-defined surface structure). For instance, when the highest hydrogen pressure (750 mbar) was used the sample temperature was at least 400 K. Under technical conditions (550 K, 25 bars) it is very likely that not only significant amounts of hydrogen are dissolved in the Pd bulk but also that a Pd hydride is formed. This certainly changes the atomic structure of the nanoparticles and may also modify their catalytic properties. It has been shown in the past that ''bulk hydrogen'' may have catalytic properties different from those of adsorbed surface hydrogen, for instance in hydrogenation[82] or hydrodechlorination reactions.[69]

IV. CONCLUSIONS

We have applied nonlinear optical sum frequency generation vibrational spectroscopy together with TDS and LEED to study adsorbate–adsorbate interactions of CO and H_2 on Pd(111) both under UHV and high-pressure (mbar) conditions. It was shown that the mutual site blocking of CO and H_2 and, therefore, the resulting adsorbate structures strongly depended on the type of gas exposure (sequential versus gas mixture) and the exposure temperature. Our results can be summarized as follows:

(a) When hydrogen was adsorbed on CO-precovered Pd(111) it was shown that CO coverages $\geqslant 0.33$ ML were very effective to prevent dissociative hydrogen adsorption, presumably by increasing the adsorption barrier because purely geometric considerations cannot explain the observed site blocking. At (total) coverages <0.33 ML hydrogen is able to adsorb on free Pd areas within CO islands of $(\sqrt{3}\times\sqrt{3})R30°$ structure (local coverage 0.33 ML).

(b) When CO was adsorbed on hydrogen-precovered Pd(111) the site-blocking ability of hydrogen strongly depended on the substrate temperature. While at 100 K hydrogen inhibited CO adsorption, at 150 K CO was able to replace hydrogen from the surface. We suggest that this effect is related to the ability of hydrogen to populate bulk Pd sites. At 100 K, the energy barrier to hydrogen bulk dissolution cannot be overcome; i.e., hydrogen stays on the surface or near the surface and blocks CO. At 150 K, the energy barrier can be overcome, allowing CO to push hydrogen to ''deeper'' Pd sites.

(c) When a 1:1 CO/H_2 mixture was adsorbed on Pd(111) both molecules reached the surface simultaneously and produced separate CO and H_2 islands. However, the resulting adsorbate structures again strongly depended on temperature. At temperatures below ~ 125 K hydrogen remained on the surface and its main effect was to block and destabilize on-top CO and to limit the coverage within CO islands to ~ 0.5 ML. Above ~ 125 K, CO was able to replace surface hydrogen which moved to Pd bulk sites and adsorbate structures identical to those of pure CO exposure were produced.

(d) When a 1:10 CO/H_2 mixture was used at high pressure (up to 55 mbar) and high temperature (300–550 K), the resulting adsorbate structures indicated CO coverages of 0.5 ML and above which strongly limit hydrogen adsorption. Under reaction conditions there were also indications of a possible surface roughening or a highly dynamic and not perfectly ordered CO phase that may facilitate CO hydrogenation.

(e) Although the temperature and CO/H_2 ratio of our mbar-pressure experiments on Pd(111) were similar to those used in catalytic studies on oxide supported Pd nanoparticles, we did not detect products. This can be understood by considering the strong blocking of hydrogen adsorption by CO under the applied conditions. Using CO/H_2 mixtures below 125 K, CO and hydrogen coexisted on the surface but, of course, this temperature is too low to drive the reaction. It is therefore reasonable to assume that oxide-supported Pd nanoparticles provide additional sites for CO hydrogenation and coadsorption studies on $Pd–Al_2O_3$ are currently performed. A further difference to technical catalysts may arise from Pd-hydride formation at hydrogen pressures well above 1 bar.

ACKNOWLEDGMENT

This work was supported by the Priority Program SPP 1091 of the German Science Foundation (DFG).

[1] T. Dellwig, G. Rupprechter, H. Unterhalt, and H.-J. Freund, Phys. Rev. Lett. **85**, 776 (2000).
[2] H. Unterhalt, G. Rupprechter, and H.-J. Freund, J. Phys. Chem. B **106**, 356 (2002).
[3] G. Rupprechter, H. Unterhalt, M. Morkel, P. Galletto, L. Hu, and H.-J. Freund, Surf. Sci. **502–503**, 109 (2002).
[4] V. V. Kaichev, I. P. Prosvirin, V. I. Bukhtiyarov, H. Unterhalt, G. Rupprechter, and H.-J. Freund, J. Phys. Chem. B **107**, 3522 (2003).
[5] M. Morkel, H. Unterhalt, M. Salmeron, G. Rupprechter, and H.-J. Freund, Surf. Sci. **532–535**, 103 (2003).
[6] H.-J. Freund, M. Bäumer, J. Libuda, T. Risse, G. Rupprechter, and S. Shaikhutdinov, J. Catal. **216**, 223 (2003).
[7] G. Rupprechter, H. Unterhalt, M. Morkel, P. Galletto, T. Dellwig, and H.-J. Freund, Vacuum **71**, 83 (2003).
[8] G. A. Somorjai and G. Rupprechter, J. Phys. Chem. B **103**, 1623 (1999).
[9] H. Conrad, G. Ertl, and E. E. Latta, J. Catal. **35**, 363 (1974).
[10] R. J. Behm, V. Penka, M.-G. Cattania, K. Christmann, and G. Ertl, J. Chem. Phys. **78**, 7486 (1983).
[11] G. A. Kok, A. Noordermeer, and B. E. Nieuwenhuys, Surf. Sci. **135**, 65 (1983).
[12] J. M. White and S. Akther, CRC Crit. Rev. Solid State Mater. Sci. **14**, 131 (1988).
[13] M. Eriksson and L.-G. Ekedahl, Appl. Surf. Sci. **133**, 89 (1998).
[14] C. Nyberg and L. Westerlund, Surf. Sci. **256**, 9 (1991).
[15] T. S. Marinova and D. V. Chakarov, Surf. Sci. **217**, 65 (1989).
[16] H. Conrad, G. Ertl, and E. E. Latta, Surf. Sci. **41**, 435 (1974).
[17] K. H. Rieder and W. Stocker, Surf. Sci. **148**, 139 (1984).
[18] S. Wilke, D. Henning, R. Löber, M. Methfessel, and M. Scheffler, Surf. Sci. **307–309**, 76 (1994).
[19] H. Okuyama, W. Siga, N. Takagi, M. Nishijima, and T. Aruga, Surf. Sci. **401**, 344 (1998).
[20] M. K. Rose, T. Mitsui, J. Dunphy, A. Borg, D. F. Ogletree, M. Salmeron, and P. Sautet, Surf. Sci. **512**, 48 (2002).
[21] T. Mitsui, M. K. Rose, E. Fomin, D. F. Ogletree, and M. Salmeron, Surf. Sci. **511**, 259 (2002).
[22] D. Hoge, M. Tüshaus, and A. M. Bradshaw, Surf. Sci. **207**, L935 (1988).
[23] H. Wang, R. G. Tobin, D. K. Lambert, G. B. Fisher, and C. L. DiMaggio, Surf. Sci. **330**, 173 (1995).
[24] J. Lauterbach, M. Schick, and W. H. Weinberg, J. Vac. Sci. Technol. A **14**, 1511 (1996).
[25] R. Zenobi, J. Xu, and J. T. Yates, Surf. Sci. **276**, 241 (1992).
[26] D. W. Goodman, J. T. Yates, and T. E. Madey, Surf. Sci. **93**, L135 (1980).
[27] G. Rupprechter, T. Dellwig, H. Unterhalt, and H.-J. Freund, Top. Catal. **15**, 19 (2001).
[28] Y. R. Shen, Nature (London) **337**, 519 (1989).
[29] A. Bandara, S. Dobashi, J. Kubota, K. Onda, A. Wada, K. Domen, C. Hirose, and S. Kano, Surf. Sci. **387**, 312 (1997).
[30] A. Tadjeddine, A. Le Rille, O. Pluchery, F. Vidal, W. Q. Zheng, and A. Peremans, Phys. Status Solidi A **175**, 89 (1999).
[31] R. Braun, B. D. Casson, C. D. Bain, E. W. M. van der Ham, Q. H. F. Vrehen, E. R. Eliel, A. M. Briggs, and P. B. Davies, J. Chem. Phys. **110**, 4634 (1999).
[32] S. Lin, A. Oldfield, and D. Klenerman, Surf. Sci. **464**, 1 (2000).
[33] C. T. Williams, Y. Yang, and C. D. Bain, Catal. Lett. **61**, 7 (1999).
[34] H. Härle, A. Lehnert, U. Metka, H. R. Volpp, L. Willms, and J. Wolfrum, Chem. Phys. Lett. **293**, 26 (1998).
[35] G. Rupprechter, Phys. Chem. Chem. Phys. **3**, 4621 (2001).
[36] M. Tüshaus, W. Berndt, H. Conrad, A. M. Bradshaw, and B. Persson, Appl. Phys. A: Solids Surf. **51**, 91 (1990).
[37] F. M. Hoffmann, Surf. Sci. Rep. **3**, 103 (1983).
[38] H. Conrad, G. Ertl, and J. Küppers, Surf. Sci. **76**, 323 (1978).
[39] H. Ohtani, M. A. Van Hove, and G. A. Somorjai, Surf. Sci. **187**, 372 (1987).
[40] W. K. Kuhn, J. Szanyi, and D. W. Goodman, Surf. Sci. Lett. **274**, L611 (1992).
[41] S. Surnev, M. Sock, M. G. Ramsey, F. P. Netzer, M. Wiklund, M. Borg, and J. N. Andersen, Surf. Sci. **470**, 171 (2000).
[42] T. Gießel, O. Schaff, C. J. Hirschmugl *et al.*, Surf. Sci. **406**, 90 (1998).
[43] D. Loffreda, D. Simon, and P. Sautet, Surf. Sci. **425**, 68 (1999).
[44] P. Galletto, H. Unterhalt, and G. Rupprechter, Chem. Phys. Lett. **367**, 785 (2003).
[45] B. Bourguignon, S. Carrez, B. Dragnea, and H. Dubost, Surf. Sci. **418**, 171 (1998).
[46] G. E. Gdowski, T. E. Felter, and R. H. Stulen, Surf. Sci. **181**, L147 (1987).
[47] W. Dong and J. Hafner, Phys. Rev. B **56**, 15 396 (1997).
[48] K. Christmann, Prog. Surf. Sci. **48**, 15 (1995).
[49] F. H. Ribeiro, C. A. Gerken, G. Rupprechter, G. A. Somorjai, C. S. Kellner, G. W. Coulston, L. E. Manzer, and L. Abrams, J. Catal. **176**, 352 (1998).
[50] A. Groß, Appl. Phys. A: Mater. Sci. Process. **67**, 627 (1998).
[51] P. A. Gravil and H. Toulhoat, Surf. Sci. **430**, 176 (1999).
[52] H. P. Bonzel and H. J. Krebs, Surf. Sci. **117**, 639 (1982).
[53] J. K. Norskov, S. Holloway, and N. D. Lang, Surf. Sci. **137**, 65 (1984).
[54] A. M. Bradshaw and F. M. Hoffmann, Surf. Sci. **72**, 513 (1978).
[55] T. E. Felter, E. C. Sowa, and M. A. Van Howe, Phys. Rev. B **40**, 891 (1989).
[56] C. Nyberg, L. Westerlund, L. Jönsson, and S. Andersson, J. Electron Spectrosc. Relat. Phenom. **54/55**, 639 (1990).
[57] M. Wilde, M. Matsumoto, K. Fukutani, and T. Aruga, Surf. Sci. **482**, 346 (2001).
[58] K. Christmann, Surf. Sci. Rep. **9**, 1 (1988).
[59] T. E. Felter, S. M. Foiles, M. S. Daw, and R. H. Stulen, Surf. Sci. **171**, L379 (1986).
[60] J. F. Paul and P. Sautet, Phys. Rev. B **53**, 8015 (1996).
[61] R. Löber and D. Henning, Phys. Rev. B **55**, 4761 (1997).
[62] W. Eberhardt, F. Greuter, and E. W. Plummer, Phys. Rev. Lett. **46**, 1085 (1981).
[63] W. Eberhardt, S. G. Louie, and E. W. Plummer, Phys. Rev. B **28**, 465 (1983).
[64] G. D. Kubiak and R. H. Stulen, J. Vac. Sci. Technol. A **4**, 1427 (1986).
[65] S. Andersson, Solid State Commun. **21**, 75 (1977).
[66] A. F. Gusovius, T. C. Watling, and R. Prins, Appl. Catal., A **188**, 187 (1999).
[67] K. Hayek, M. Fuchs, B. Klötzer, W. Reichl, and G. Rupprechter, Top. Catal. **13**, 55 (2000).
[68] P. J. Berlowitz and D. W. Goodman, J. Catal. **108**, 364 (1987).
[69] G. Rupprechter and G. A. Somorjai, Catal. Lett. **48**, 17 (1997).
[70] G. C. Cabilla, A. L. Bonivardi, and M. A. Baltanas, Catal. Lett. **55**, 147 (1998).
[71] C. Chinchen, P. J. Denny, J. R. Jennings, M. S. Spencer, and K. C. Waugh, Appl. Catal. **36**, 1 (1988).
[72] G. W. Bridger and M. S. Spencer, in *Catalyst Handbook*, edited by M. V. Twigg (Wolfe, London, 1989), pp. 441–468.
[73] Y. A. Ryndin, R. F. Hicks, A. T. Bell, and Y. I. Yermakov, J. Catal. **70**, 287 (1981).
[74] W. Reichl, G. Rosina, G. Rupprechter, C. Zimmermann, and K. Hayek, Rev. Sci. Instrum. **71**, 1495 (2000).
[75] B. Klötzer, W. Unterberger, and K. Hayek (private communication).
[76] A. Gotti and R. Prins, J. Catal. **175**, 302 (1998).
[77] A. Gotti and R. Prins, Catal. Lett. **37**, 143 (1996).
[78] R. F. Hicks and A. T. Bell, J. Catal. **90**, 205 (1984).
[79] S. Shaikhutdinov, M. Heemeier, M. Bäumer, T. Lear, D. Lennon, R. J. Oldman, S. D. Jackson, and H.-J. Freund, J. Catal. **200**, 330 (2001).
[80] C. Sellmer, R. Prins, and N. Kruse, Catal. Lett. **47**, 83 (1997).
[81] R. F. Hicks and A. T. Bell, J. Catal. **91**, 104 (1985).
[82] A. D. Johnson, K. J. Maynard, S. P. Daley, Q. Y. Yang, and S. T. Ceyer, Phys. Rev. Lett. **67**, 927 (1991).